



Nonlinear wave transformations and randomness

S. Beji

To cite this article: S. Beji (2019) Nonlinear wave transformations and randomness, Coastal Engineering Journal, 61:4, 590-598, DOI: [10.1080/21664250.2019.1672126](https://doi.org/10.1080/21664250.2019.1672126)

To link to this article: <https://doi.org/10.1080/21664250.2019.1672126>



Published online: 27 Sep 2019.



Submit your article to this journal [↗](#)



Article views: 27



View related articles [↗](#)



View Crossmark data [↗](#)

TECHNICAL NOTE



Nonlinear wave transformations and randomness

S. Beji

Faculty of Naval Architecture and Ocean Engineering, Istanbul Technical University, Istanbul, Turkey

ABSTRACT

Variations of raw spectral estimates of ocean waves with quite different sea states are examined for confirming their fitness to theoretical chi-square distribution with two degrees of freedom. A hypothetical numerical experiment is devised and histograms of spectral variability for artificially produced initial wave spectrum of constant shape undergoing nonlinear transformations are computed and compared with the chi-square distribution. As the nonlinear energy transfer among wave components develops, the histograms of spectral variability, initially constant, evolve to the exponentially decaying chi-square form. Once the variability distribution attains the exponential form it remains so regardless of the change in wave field characteristics, as for waves becoming linear by propagating into deeper regions. Irreversible nonlinear wave transformations not only redistribute the spectral energy broadly but also do it by imparting a variability to spectral components which accords with the chi-square distribution, indicating true randomness.

ARTICLE HISTORY

Received 13 August 2018

Accepted 11 September 2019

KEYWORDS

Nonlinearity; randomness; spectral variability; chi-square distribution

1. Introduction

Variations in spectral representations of different segments of a given wave record are usually smoothed out by combined application of segment and frequency averaging. Resulting spectral forms do look quite smooth; however, any possible concern which might arise from sharp variations in individual raw spectra is likewise washed out. Apparently, Donelan and Pierson (1983) were the first to question the reliability of main wave parameters obtained from the smoothed spectral estimates and examined the problem from various aspects. Uncertainties due to spectral variability in practically required quantities such as significant wave height and peak period, were estimated. An important verification was that the spectral variability followed the chi-square distribution. The chi-square distribution, introduced by Pearson (1900), measures the goodness of fit of any given distribution to random variables. In other words, it may be interpreted as an indicator of true randomness.

On the other hand, a related subject; namely, sampling variability effects, or statistical uncertainty arising from limited data has also received some attention (see, for instance, Forristall et al. 1996; Hagen 2007; Bitner-Gregersen and Magnusson 2014).

Beji and Nadaoka (1998) examined the spectral variations and their relevance to wave force estimations. The main purpose of the work was to analyze the variability of wave forces acting on a sea structure. Also, some interesting aspects of nonlinear energy exchange among spectral components were reported

as a side product. The present work revisits Beji and Nadaoka (1998), while placing a strong emphasize on a possible connection between nonlinear wave energy exchanges and randomness.

The first part of this study contains analysis of field data of Nakamura and Katoh (1992) with respect to the variability of raw spectral estimates and the fitness of this variability to the chi-square distribution. Data representing characteristically different sea states are selected especially to demonstrate that the fitness of spectral variability to the chi-square distribution is independent of wave characteristics. This observation also implies that the lack of conformity to the Gaussian distribution does not affect the agreement with the chi-square distribution.

The second part of the work devises a numerical experiment involving simulation of nonlinear wave transformations over a parabolic hump. Wave parameters are adjusted such that growth and strengthening of bound waves are promoted in the shoaling region. As bound waves gain strength the energy exchange among different wave components increase and take place according to phase mismatch values which diminish in shallow waters (Madsen and Sørensen 1993). In turn, phase mismatch controlled rapid energy exchanges among wave components give rise to sharp differences in their energy contents. For a wave field with unvarying initial spectral shape, these fluctuations spread over the entire frequency band and cause considerable variations in raw spectral estimates. With sufficient energy exchange,

histograms of spectral variations are observed to approach the chi-square distribution.

The study then concludes that nonlinear energy exchanges among wave components impart a spectral variability in accord with the chi-square distribution, which indicates a truly random process.

2. Spectral variability histograms of field measurements

Nakamura and Katoh (1992) conducted field observations of waves at the Hazaki Oceanographical Research Facility, Kashima, Japan. The field observations took place at a beach facing the Pacific Ocean. Seven out of 10 ultrasonic wave gauges were installed on the 427 m-long pier while the remaining three were deployed at water depths of 9 m (Station 8), 14 m (Station 9), and 24 m (Station 10), located at 1300 m, 2100 m, and 3200 m from the shoreline. Figure 1 shows a schematic view of the beach profile and the locations of Stations 5–10. Two separate groups of measurements were done; the first from February 25 to March 1, 1989, and the second from October 5 to 9, 1989. Here, the data from the first group of measurements are utilized.

In the first measurement group during the first recording on February 25, 1989, the sea state was relatively calm with significant wave height $H_s = 1.5$ m and period $T_s = 4.8$ s at the farthest offshore station (Station 10). On February 26, 1989 an atmospheric depression passed nearby the measurement location and created a high sea state with swell. Thus, in the aftermath of the storm, the records on February 28, 1989 revealed approximately $H_s = 2.2$ m and $T_s = 12.4$ s for Station 10. While waves recorded at Stations 5–7 were either breaking or broken, waves observed at Stations 8–10, were generally unaffected by depth-induced breaking.

The data of February 25 and 28, 1989 are used for examining the spectral variations of the field data. The first of these represent relatively mild sea conditions while the second one is typically a swell data recorded after a storm. These characteristically different data sets are especially selected so that the effects of these differences, if any, on the spectral variability could be observed.

Computations of spectral variability follow exactly the method outlined in Donelan and Pierson (1983); only the numerical values (e.g. the running averages, number of segments, etc.) differ. For each station, data were first segmented into $M = 12$ groups of 1024 points and Fourier transformed. From 512 unique Fourier pairs, the first $N = 256$ components, which included the frequency range 0.0 – 1.0 Hz, were considered adequate to contain most wave energy and therefore the computations for spectral variations were done using the first 256 transformed pairs.

For each set comprising the Fourier components a_n and b_n for $n = 1, \dots, N$, the Fourier amplitudes $C_n^2 = \frac{1}{2}(a_n^2 + b_n^2)$ were frequency smoothed by a five-point running average $2L + 1 = 5$:

$$\bar{C}_{nm}^2 = \frac{1}{2L + 1} \sum_{i=n-L}^{n+L} C_{im}^2 \quad (1)$$

where $m = 1, \dots, M$ indicates the segment number. Using the frequency smoothed values, segment averaging was performed for $M = 12$:

$$\hat{C}_n^2 = \frac{1}{M} \sum_{m=1}^M \bar{C}_{nm}^2 \quad (2)$$

which, in turn, are used to compute the spectral estimates $\hat{S}_n = \hat{C}_n^2 / \Delta f$ with $2 \times 5 \times 12 = 120$ degrees of freedom. Here, $\Delta f = 1/\Delta t$, and $\Delta t = 0.5$ s the sampling interval. It must be emphasized

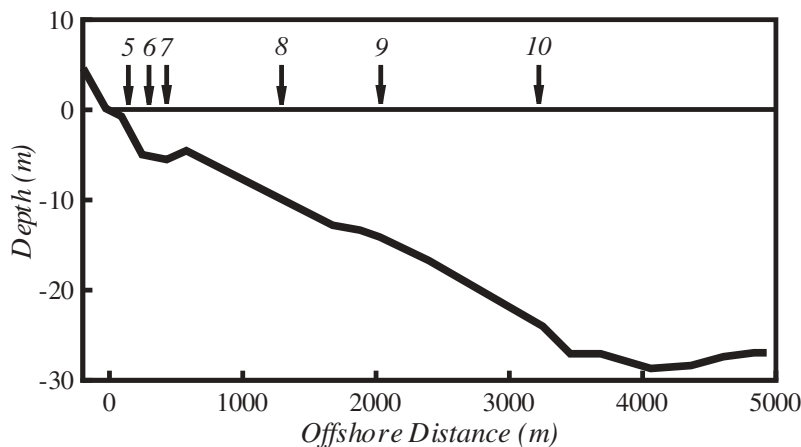


Figure 1. Schematic view of beach profile and measurement stations 5–10 of Nakamura and Katoh (1992).

that \hat{S}_n is only an estimate of the true spectrum with definite uncertainty.

For a Gaussian process, the 90% confidence level for the estimated spectral variance with 120 degrees of freedom is computed as (Bendat and Piersol 1971, 114)

$$P\left(\frac{120\hat{S}_n^2}{\chi_{120;0.05}^2} < S_n < \frac{120\hat{S}_n^2}{\chi_{120;0.95}^2}\right) = 0.90 \quad (3)$$

in which, for simplicity, $DOF = 120$ is used instead of $DOF - 1 = 119$. Substituting $\chi_{120;0.95}^2 = 95.70$, $\chi_{120;0.05}^2 = 146.57$ gives

$$P(0.82\hat{S}_n^2 < S_n < 1.25\hat{S}_n^2) = 0.90. \quad (4)$$

Accordingly, the true spectrum is known to within $\pm 25\%$ or a range of $18\% + 25\% = 43\%$ at the 90% confidence level.

Figure 2(a) is a raw spectral estimate $C_n^2/\Delta f$ based on FFT of a single segment with 1024 data points for the measurement of February 28, 1989 at Station 10. Figure 2(b) is the running and segment averaged spectral estimate $\hat{S}_n = \hat{C}_n^2/\Delta f$ for the same measurement. The 90% confidence limits are indicated by dash-dot lines. Comparing Figure 2(a) with 2(b) quite clearly reveals the appreciable variations between a single realization and

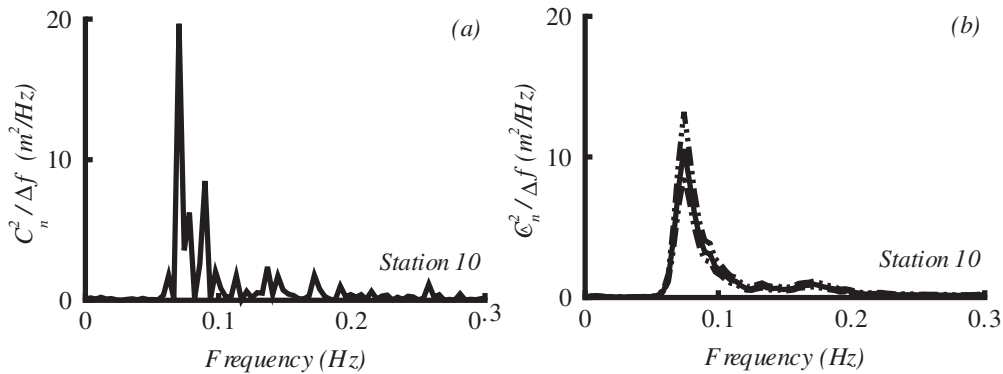


Figure 2. (a) Raw spectral estimate for a single data segment with 2 DOF. (b) Spectral estimate and 90% confidence limits (dash-dot lines) for 12 segment averaging and five-point frequency smoothing with 120 DOF. February 28, 1989 data.

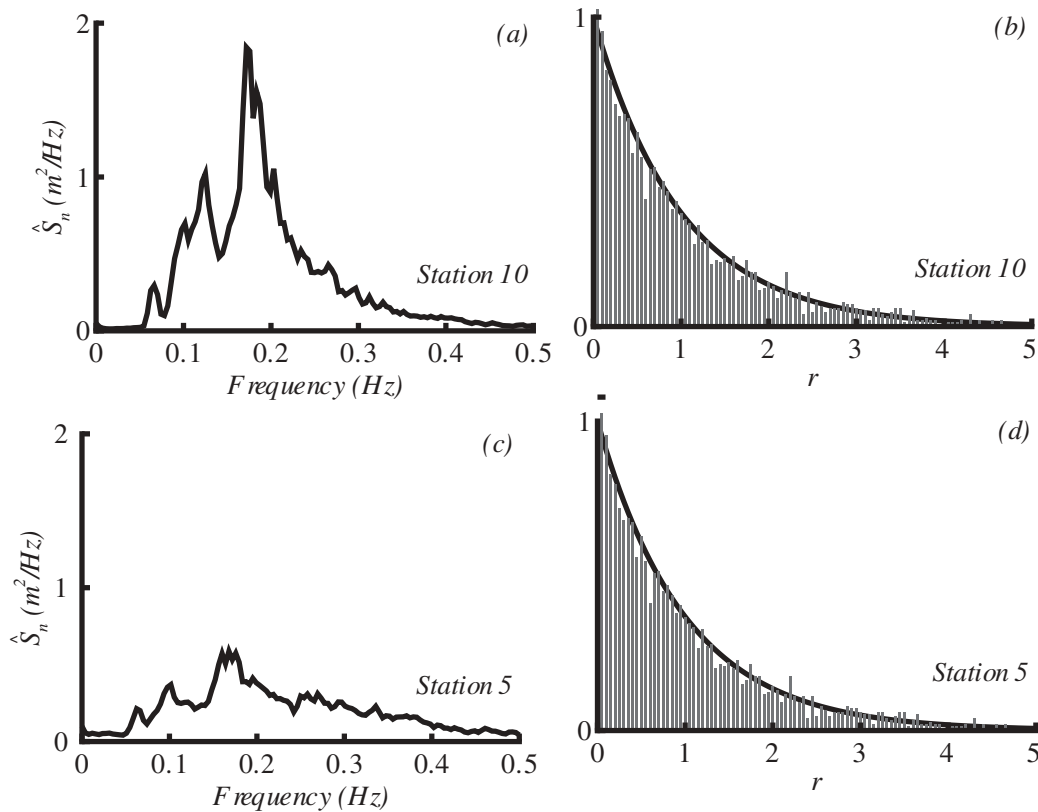


Figure 3. Left column: the smoothed average spectral estimates with 120 DOF. Right column: Histograms of the ratio, r , of raw FFT spectral estimates to the smoothed average spectral estimates for the class interval 0.05. The solid line is the theoretical $\exp(-r)$ curve. February 25, 1989 data.

smoothed and averaged spectrum. Hypothetically, these variations may be quantified by the random variable $r = C_n^2 / S_n \Delta f$. However, since the true spectrum S_n is not known, as an acceptable approximation, the estimate \hat{S}_n computed by five-point running average over frequency and an average of 12 segments of available data may be used. Thus, the random variable r is redefined as $C_n^2 / \hat{S}_n \Delta f$ and used to establish histograms for testing randomness of the spectral variations (Donelan and Pierson 1983). Theoretically, r is expected to be distributed according to $\exp(-r)$, which is the chi-square distribution with two degrees of freedom.

Calculations were carried out for the data of 25 and February 28, 1989 using 12 segments with 256 pairs of Fourier components encompassing the frequency range 0.0 – 1.0 Hz and resulting in 3072 different r values. Strictly speaking, near zero values of \hat{S}_n should have been excluded to avoid numerical errors; however, no problems were run into and therefore all \hat{S}_n values were used. Spectral estimates are given in Figure 3(a,c) while corresponding histograms for the 3072 values of r for a class interval 0.05 wide are shown in Figure 3(b,d) over the range $0 < r < 5$. Each histogram has been normalized by its value in the first interval (0.00 – 0.05). Figure 4(a–d) show the same computations for the data of February 28, 1989.

Differences in sea states of February 25 and 28, 1989 are obvious from the distinctly different spectral

characteristics, revealed prominently in the energy content and frequency range of waves depicted in Figures 3 and 4. Despite these remarkable dissimilarities in spectral forms, the histograms of spectral variability are hardly different from each other. The only exception is Figure 4(d), where the wave energy is greatly consumed by breaking as observed from Figure 4(c). Nevertheless, the histograms are generally in good accord with the theoretical $\exp(-r)$ curve, implying that randomness of a natural sea state is not affected by its defining characteristics such as mean wave height and period. This preliminary investigation of the random nature of different sea states and their quantitative identification by the chi-square distribution serves as a basis to carry out similar calculations for artificially produced random wave transformations.

3. A numerical simulation for a hypothetical case

The fitness of spectral variations to the exponential chi-square distribution is regarded as a measure of randomness of the spectral variations. For wave fields with different wave characteristics, relatively linear waves of February 25, 1989 data versus highly nonlinear waves of February 28, 1989 data, the fitness of spectral variations to the exponential form is confirmed. This natural property of sea waves, which is basically independent of their

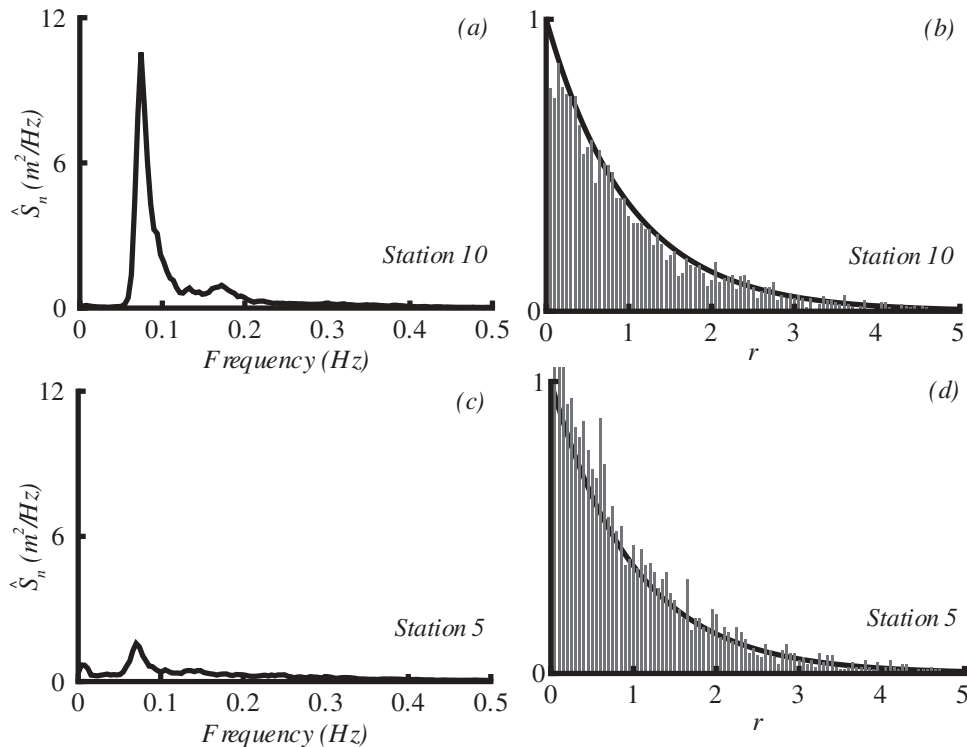


Figure 4. Left column: the smoothed average spectral estimates with 120 DOF. Right column: Histograms of the ratio, r , of raw FFT spectral estimates to the smoothed average spectral estimates for the class interval 0.05. The solid line is the theoretical $\exp(-r)$ curve. February 28, 1989 data.

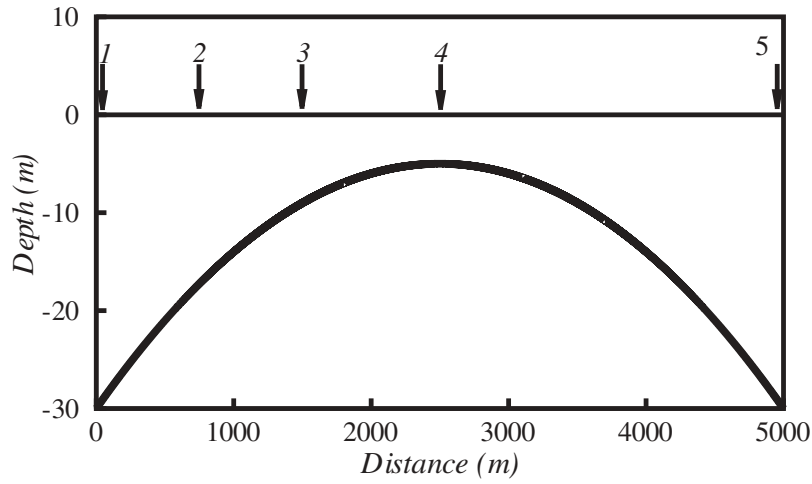


Figure 5. Bathymetry for hypothetical numerical experiment and locations of monitoring stations 1–5.

characteristics, is now examined for artificially generated waves as an attempt to disclose its source.

A hypothetical numerical experiment is devised for a unidirectional random wave field propagating over a parabolic shoal. The computational domain is 5000 m long and the water depth at the beginning of the domain is 30 m, which reduces to 5 m in the middle of the domain and then increases to 30 m again as shown in Figure 5. An approximate average slope as computed from $(30 - 5)/2500 = 1/100$, which is quite gentle, may be attributed to each half of the domain. For monitoring the evolution of the wave spectra and spectral variations, five stations are considered. Station 1 and Station 5 are placed, respectively, at the beginning 0 m and end 5000 m of the domain while Stations 2–4 are located, respectively, at 750 m, 1500 m, and 2500 m from the beginning of the domain.

Incident wave field in the deep region is assumed to be a Bretschneider-type spectrum (Bretschneider 1959), which is defined in terms of the significant wave height H_s and peak period T_p as

$$S(f) = \frac{5H_s^2}{16f_p} \frac{1}{(f/f_p)^5} \exp \left[-\frac{5}{4} \left(\frac{f}{f_p} \right)^{-4} \right] \quad (5)$$

where $f_p = 1/T_p$ and f is the varying frequency. For promoting second-order shallow water (long wave) interactions over the hump the peak wave period is taken as $T_p = 10$ s so that $h/L_p \simeq 1/15$ over the top of the bar. To decide for the incident significant wave height, a generalized wave non-linearity parameter (Beji 1995) is employed

$$\varepsilon = \frac{gH}{C_p^2} \quad (6)$$

where g is the gravitational acceleration, H the wave height, and C_p the linear theory phase velocity. Note that this non-linearity parameter embodies the shallow $C_p^2 = gh$, $\varepsilon = H/h$ and deep water $C_p^2 = g/k$, $\varepsilon = kH$ cases as limiting values therefore has the advantage of

applicability over the entire range of relative water depths. Further, setting ε to a definite maximum value 0.88 results in Miche's wave breaking criterion (Miche 1951).

The incident significant wave height is determined by ensuring a moderately energetic incident wave field while avoiding breaking in the shallowest region over top of the shoal. Thus, the non-linearity parameter is set to a relatively moderate value $\varepsilon = 0.1$ at the beginning of the domain so that for $h = 30$ m water depth the phase velocity being $C_p = 13.7$ m/s, from Equation (6) the incident significant wave height is calculated as $H_s = 1.9$ m. From the conservation of energy flux the significant wave height over top of the shoal at $h = 5$ m water depth is estimated as $H_s = 2.3$ m and the phase velocity $C_p = 6.8$ m/s so that $\varepsilon = gH_s/C_p^2 \simeq 0.5$, an appreciable value. Wave heights computed using the spectra ($H_s = 4\sqrt{m_0}$) obtained from the nonlinear numerical simulation confirm the wave heights estimated from the energy flux concept. It must be emphasized that as various similar numerical experiments revealed, neither the devised bathymetry nor the wave parameters are unique to obtain the general results that follow; the crucial point is to arrange a case where non-linear wave evolutions take place.

For numerical simulations, a generalized KdV-type equation valid for uneven water depths is employed (Beji 2016),

$$\begin{aligned} \zeta_t + C\zeta_x + \frac{3}{4}Ch^{-1}(\zeta^2)_x - \frac{(1+2\beta)}{6}Ch^2\zeta_{xxx} \\ - \frac{(1+\beta)}{3}h^2\zeta_{xxt} + \frac{1}{4}Ch^{-1}h_x\zeta - \frac{(15+32\beta)}{24}Chh_x\zeta_{xx} \\ - \frac{5(1+\beta)}{6}hh_x\zeta_{xt} = 0 \end{aligned} \quad (7)$$

where ζ is the free surface displacement, h the water depth, $C = \sqrt{gh}$ the non-dispersive shallow water wave celerity and β a nondimensional dispersion

parameter. Subscripts x and t indicate partial differentiation with respect to space and time, respectively. Equation (7) embodies all the known KdV-type equations as special cases. For constant depth, setting $\beta = -1$ results in the original Korteweg and de Vries (1895) equation while $\beta = -1/2$ gives the so-called regularized KdV equation of Benjamin, Bona, and Mahony (1972). On the other hand, $\beta = -1/20$ produces a wave equation with dispersion relationship corresponding to the [2/2] Padé approximant of the exact dispersion relation. Finally, for $\beta = 0$ the linear shoaling characteristics of the equation are in exact agreement with those determined from the constancy of energy flux.

Setting $\beta = 0$, Equation (7) was solved numerically by spectral method as described in Beji (2016). Accordingly, spectral amplitudes at discrete frequencies were introduced at the incident boundary (Station 1) and computations were carried out in marching-forward manner till the desired last point (Station 5). Spectral method has the advantage of not requiring any outgoing boundary condition.

The incident wave field was introduced as a Bretshneider-type spectrum with 256 Fourier pairs with $\Delta f = f_c/256 = 1.953 \times 10^{-3} \text{ Hz}$, where the cutoff frequency f_c was set to $6f_p = 6/T_p$, f_p being the peak frequency of the spectrum. Twelve realizations with constant spectral shape but different random phase assignments were performed. Frequency smoothing was done by five-point running average while segment averaging was performed with 12 segments. Thus, the statistical values given in the previous section for measurements apply to the analysis of numerical simulations as well. Use of different running-average points and realizations has been confirmed to cause no appreciable effect on the overall results. For instance, a computation with seven-point running average and 16 realizations gave only relatively more smoothed spectra due to higher frequency averaging but basically the same histograms.

In Figure 6, on the left column, the computed spectra obtained after frequency smoothing and ensemble averaging are shown at the locations 0 m, 750 m, 1500 m, 2500 m, and 5000 m which, respectively, correspond to the water depths 30 m, 17.25 m, 9 m, 5 m, and 30 m. The corresponding spectral variability histograms are shown on the right column.

Since spectral heights for all realizations at Station 1 are purposely imposed as constant, Figure 6(a), the corresponding variability histogram in Figure 6(b) has a single spike at $r = 1$. As the waves travel over shallower depths, increasing non-linearity begins slowly manifesting itself as observed from the not-quite-smooth form of the spectrum at Station 2, Figure 6(c). The spectral variability is initiated but its appearance is obviously very different from the

theoretical chi-square distribution. Wave spectrum at Station 3 shows obvious signs of non-linearity with increased energy at lower and upper frequency regions, Figure 6(e), while the spectral variability is appreciably broader and adjusting itself to the chi-square form, Figure 6(f). Station 4, being the shallowest station with 1/6th of the initial water depth, exhibits a spectrum with broadband energy distribution, Figure 6(g), and the spectral variability histogram has attained a distribution which follows the theoretical chi-square curve quite closely, Figure 6(h). Farther at Station 5, waves are in relatively deep water again and their non-linearity is quite diminished as it is obvious from the area under the spectrum, Figure 6(i). However, the nonlinear energy transfer over the shallow region has accomplished the redistribution of energy over the entire band of the spectrum and the spectrum is drastically different from its former shape in Figure 6(a). Finally, the spectral variability, being randomized by nonlinear energy exchanges and having attained a chi-square form, maintains its chi-square distribution even in deeper waters where waves become linear again, Figure 6(j).

This entire process appears to be quite in line with Hasselmann's long-standing arguments concerning nonlinear irreversible energy transfer due to nonlinear near-resonant interactions of deep water waves (Hasselmann 1962, 1963a, 1963b). The corresponding process for shallow water waves, as applicable to the present case, has been explained in detail quite clearly in Madsen and Sørensen (1993). Compared to the third-order deep water interactions (four wave components) the second-order shallow water interactions (three wave components) are stronger and the evolution of the wave field is accomplished at a faster rate in shorter distances: Station 4 is less than 25 mean wavelengths from Station 1 and for a similar experimental case of wave propagation over a bar (Beji and Battjes 1993), the main energy exchange takes place within three mean wavelengths for relatively long random waves. Evolutions of spectral shape clearly show the "irreversible tendency to spread the wave energy evenly over all wavenumbers", quoting Hasselmann (1967) verbatim. Besides that the spectral variability histograms reveal the randomizing nature of this energy distribution mechanism. Energy distribution progress takes place in such a fashion that the spectral variability eventually attains a chi-square form and retains this property even after the wave field becomes linear as observed for Station 5, which is especially designated to be in deep water. The results obtained from the field data of February 25, 1989 (mostly linear) and February 28, 1989 (mostly nonlinear) are parallel in the sense that the chi-square-type-spectral-variability is independent of wave field characteristics.

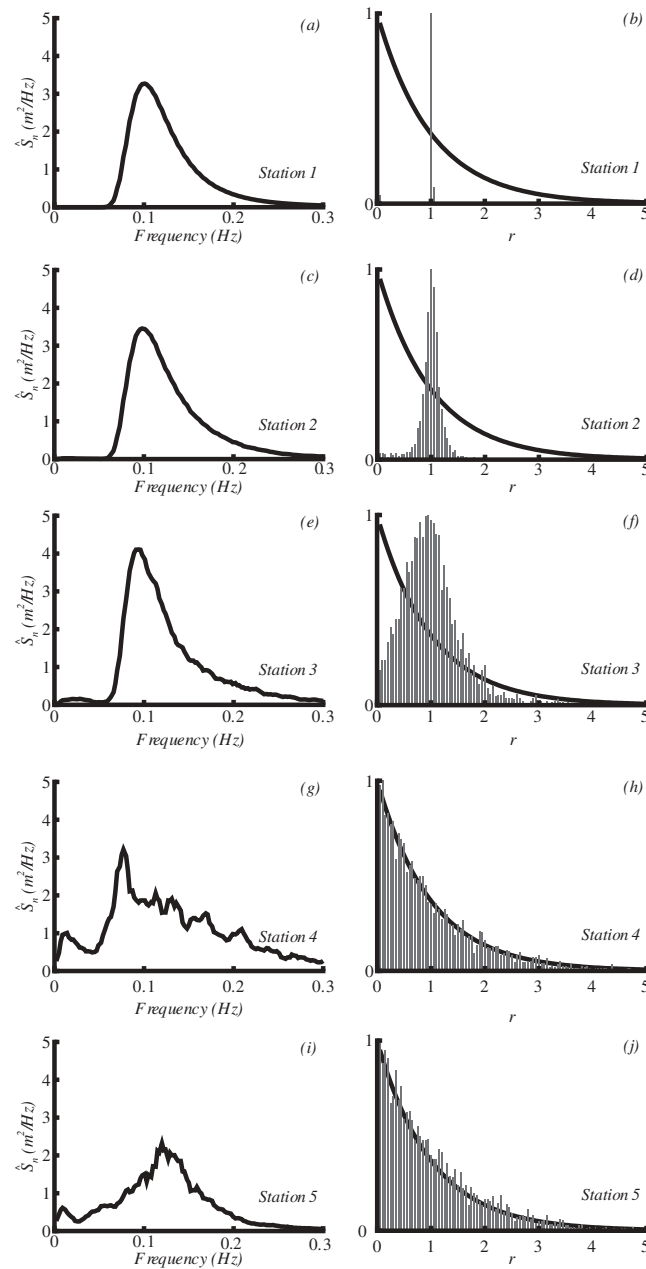


Figure 6. Nonlinear computations. Left column: the smoothed average spectral estimates with 120 DOF. Right column: Histograms of the ratio, r , of raw FFT spectral estimates to the smoothed average spectral estimates for the class interval 0.05. The solid line is the theoretical $\exp(-r)$ curve.

On the other hand, when the numerical experiment is carried out using the linearized version of Equation (7) with $(\zeta^2)_x$ term dismissed, the results look quite different as shown in Figure 7(a–f). The spectral shape at the end of the domain, Station 5, is now exactly the same as the incident wave spectrum at Station 1. The form of wave spectrum changes due to linear shoaling but histograms of spectral variations remain unchanged, as in Figure 6(b), for all the stations.

In closing, the numerical simulations demonstrate clearly that nonlinear wave interactions are capable of imparting variability to a wave spectrum of initially constant form. The precise order

(i.e. second, third) of the nonlinear mechanism is immaterial as long as it facilitates redistribution of energy among spectral components. After sufficient energy exchange the eventual spectral variability histogram is expected to approach the chi-square form; namely, a truly random process. Finally, in this randomization process, the shape of bathymetry is not important at all since a similar numerical test, previously conducted over a constant slope, gave virtually the same results (Beji and Nadaoka 1998). The most important thing is to promote the nonlinear energy exchange among spectral components by making amplitudes large enough.

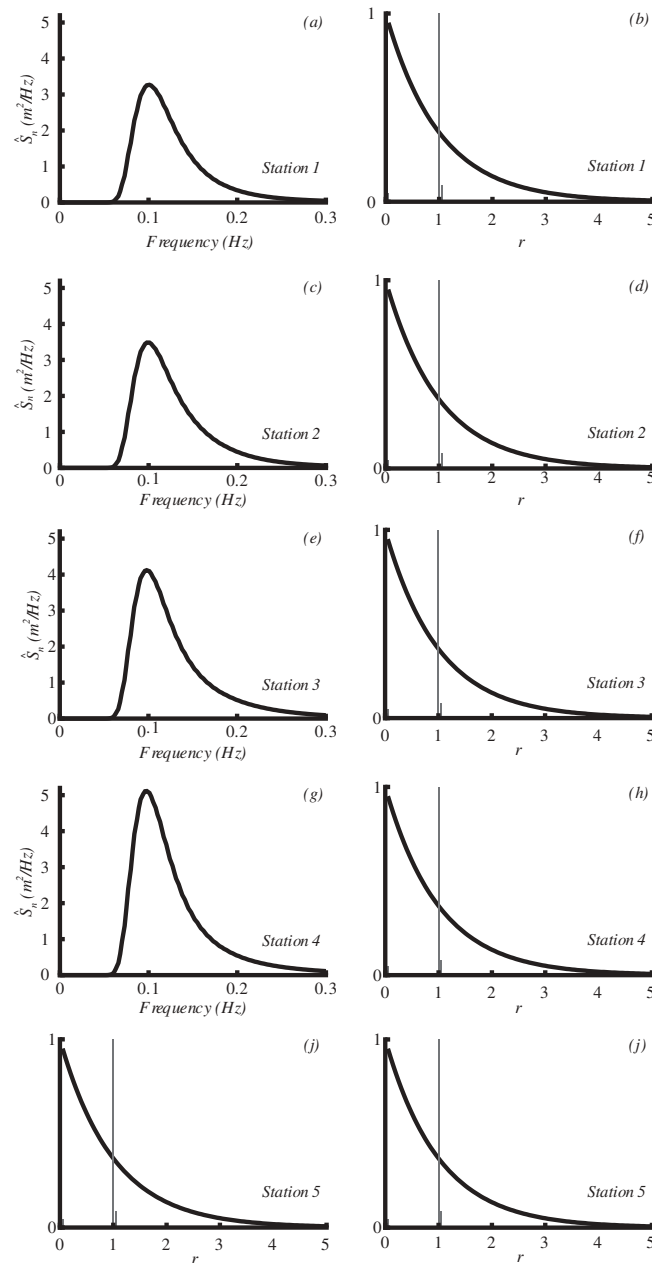


Figure 7. Linear computations. Left column: the smoothed average spectral estimates with 120 DOF. Right column: Histograms of the ratio, r , of raw FFT spectral estimates to the smoothed average spectral estimates for the class interval 0.05. The solid line is the theoretical $\exp(-r)$ curve.

4. Concluding remarks

Spectral variability analysis of a field data comprising distinctly different sea states (basically linear February 25, 1989 data and highly nonlinear February 28, 1989 data) has confirmed, regardless of the wave field characteristics, the tenability of the customary presumption that the spectral variability histograms follow the exponentially decaying chi-square distribution. A hypothetical numerical experiment has been devised to examine the spectral variability of an initially constant spectral form undergoing nonlinear evolutions over bathymetry. Histograms of spectral variability reveal that such a constant spectral form gradually attains

a variability, which is in good agreement with the chi-square distribution. The spectral variability, once gained, is maintained even if the wave field becomes linear by moving into deeper waters or breaking. Nonlinear wave interactions may be responsible not only for energy redistribution among spectral components but also for the truly random spectral variability observed in ocean waves.

Acknowledgments

The author is indebted to Dr. K. Katoh and S. Nakamura for supplying the field data.

Disclosure statement

No potential conflict of interest was reported by the author.

ORCID

S. Beji  <http://orcid.org/0000-0002-1927-9262>

References

- Beji, S. 1995. "Note on a Nonlinearity Parameter of Surface Waves." *Coastal Engineering* 25: 81–85. doi:10.1016/0378-3839(94)00031-R.
- Beji, S. 2016. "Improved Korteweg & De Vries Type Equation with Consistent Shoaling Characteristics." *Coastal Engineering* 109: 128–133. doi:10.1016/j.coastaleng.2015.10.009.
- Beji, S., and J. A. Battjes. 1993. "Experimental Investigation of Wave Propagation over a Bar." *Coastal Engineering* 19: 151–162. doi:10.1016/0378-3839(93)90022-Z.
- Beji, S., and K. Nadaoka. 1998. "Variations in Nonlinearly Evolved Nearshore Spectra and Their Significance in the Estimation of Wave Forces." In *Proceedings of the 26th International Conference on Coastal Engineering*, 682–691. Copenhagen, Denmark.
- Bendat, J. S., and A. G. Piersol. 1971. *Random Data: Analysis and Measurement Procedures*. New York: John Wiley & Sons.
- Benjamin, T. B., J. L. Bona, and J. J. Mahony. 1972. "Model Equations for Long Waves in Nonlinear Dispersive Systems." *Philosophical Transactions of the Royal Society A* 272: 47–78. doi:10.1098/rsta.1972.0032.
- Bitner-Gregersen, E. M., and A. K. Magnusson. 2014. "Effect of Intrinsic and Sampling Variability on Wave Parameters and Wave Statistics." *Ocean Dynamics* 64: 1643–1655. doi:10.1007/s10236-014-0768-8.
- Bretschneider, C. L. 1959. "Wave Variability and Wave Spectra for Wind-generated Gravity Waves." Technical Memo. No. 188, Beach Erosion Board, U. S. Army Corps of Engns.
- Donelan, M., and W. J. Pierson. 1983. "The Sampling Variability of Estimates of Spectra of Wind-generated Gravity Waves." *Journal of Geophysical Research* 88: 4381–4392. doi:10.1029/JC088iC07p04381.
- Forristall, G. Z., J. C. Heideman, I. M. Leggett, B. Roskam, and L. Vanderschuren. 1996. "Effect of Sampling Variability on Hindcast and Measured Wave Heights." *Journal of Waterway, Port, Coastal, and Ocean Engineering* 122: 216–225. doi:10.1061/(ASCE)0733-950X(1996)122:5(216).
- Hagen, Ø. 2007. "Wave Distributions and Sampling Variability." In *Proceedings of the 26th International Conference on Offshore Mechanics and Arctic Engineering*. San Diego, CA, USA.
- Hasselmann, K. 1962. "On the Non-linear Energy Transfer in a Gravity-wave Spectrum. Part 1. General Theory." *Journal of Fluid Mechanics* 12: 481–500. doi:10.1017/S0022112062000373.
- Hasselmann, K. 1963a. "On the Non-linear Energy Transfer in a Gravity Wave Spectrum. Part 2. Conservation Theorems; Wave-particle Analogy; Irreversibility." *Journal of Fluid Mechanics* 15: 273–281. doi:10.1017/S0022112063000239.
- Hasselmann, K. 1963b. "On the Non-linear Energy Transfer in a Gravity-wave Spectrum. Part 3. Evaluation of the Energy Flux and Swell-sea Interaction for a Neumann Spectrum." *Journal of Fluid Mechanics* 15: 385–398. doi:10.1017/S002211206300032X.
- Hasselmann, K. 1967. "Nonlinear Interactions Treated by the Methods of Theoretical Physics (with Application to the Generation of Waves by Wind)." (A Discussion on *Nonlinear Theory of Wave Propagation in Dispersive Systems*.) *Proceedings of the Royal Society of London. Series A* 1456 (299): 77–100.
- Korteweg, D. J., and G. de Vries. 1895. "On the Change of Form of Long Waves Advancing in a Rectangular Canal, and on a New Type of Long Stationary Waves." *Philosophical Magazine* 39: 422–443. doi:10.1080/14786449508620739.
- Madsen, P. A., and O. R. Sørensen. 1993. "Bound Waves and Triad Interactions in Shallow Water." *Ocean Engineering* 20: 359–388. doi:10.1016/0029-8018(93)90002-Y.
- Miche, R. 1951. "Le Pouvoir Reflechissant Des Ouvrages Maritimes Exposés À L'action De La Houle." *Annales Ponts Chaussées* 121: 285–319.
- Nakamura, S., and K. Katoh. 1992. "Generation of Infragravity Waves in Breaking Process of Wave Groups." In *Proceedings of the 27th International Conference on Coastal Engineering*, 990–1003. Venice, Italy.
- Pearson, K. 1900. "On the Criterion that a Given System of Deviations from the Probable in the Case of a Correlated System of Variables Is Such that It Can Be Reasonably Supposed to Have Arisen from Random Sampling." *Philosophical Magazine* 5 (50): 157–175. doi:10.1080/14786440009463897.